Optical Properties of Semiconductors
Universität Konstanz

Optical Stark Effect

Michael Körber (michael.koerber@uni-konstanz.de)

July 12, 2011

Abstract

The excitonic optical Stark effect describes a light field induced Stark effect in semiconductors, i.e. a shift in the optical absorption in the presence of an external light field. By using analogies to the known optical Stark effect in two-level atoms and the semiconductor Bloch equations results for the blueshift in transition energies are derived in the case of semiconductors. This is first performed in a quasi stationary approximation to find the general effects that occur. In a more detailed second step, the dynamic effects, that happen due to the fast dephasing times in semiconductors are considered. By analytically deriving the change in susceptibility, a blueshift in the transition energy is found, leading to a optical Stark effect in semiconductors, which has been experimentally confirmed.

Contents

1 Introduction

The Stark effect describes a splitting of energy levels of either a atom, molecule or semiconductor in an external electric field. A subtype is the optical Stark effect, where the external electric field is provided by a light field. In the following, I describe the optical Stark effect in a two-level atom to provide a basic understanding of the process. This is used to point out the differences and similarities between the effects in an atom and a semiconductor. The splitting of the energy levels in a two level atom delivers the basis for a description of the optical Stark effect in a semiconductor.
A semiconductor is a much more complicated system to observe such an effect, because any induced polarization decays within a time scale of femtoseconds. That is why this effect first could be observed in the 1980s when development of femtosecond lasers allowed the study of such short time scales. For simplicity, we start with an analysis of a semiconductor in the quasi-stationary approximation. One can see that this approximation is not valid due to the short coherence times in semiconductors, but one can nevertheless find basic similarities to the optical Stark effect in a tow level atom that deliver some detail information. Then in a second step the dynamics of the optical Stark effect in semiconductors, or excitonic optical Stark effect, is studied. As a result a splitting is found that becomes manifest in a blueshift of the exciton energy.

2 Optical stark effect in two-level atoms

This chapter deals with the optical stark effect in a atom, that is assumed to have two energy levels. In section 2.1 we calculate the energy levels and the huge dependence of the wave function of the atom, perturbed by the interaction with a light field. In section 2.2 we repeat the same calculation in second quantization to connect with the description that is used for the semiconductor in section 3 and obtain the same results as expected.

2.1 Atom in light field

This section shows the simplest description of the optical Stark effect. The model used here considers no damping nor any other effect that is not essential to find the splitting in energy levels. Therefore, one uses an atom with only one electron and two energy levels ϵ_1 and ϵ_2 with $\epsilon_1 < \epsilon_2$. This atom is perturbed by a light field $\mathcal{E}(t)$ what leads to an interaction Hamiltonian of

$$\mathcal{H}_I(t) = -ex\mathcal{E}(t) = -d\mathcal{E}(t) \tag{1}$$

with d the dipole moment. The time-dependent wave function of this atom is then given by

$$\psi(\boldsymbol{r}, t) = \sum_n a_n(t) e^{-i\epsilon_n t} \psi_n(\boldsymbol{r}) \tag{2}$$

where $\psi_n(\boldsymbol{r})$ are the stationary eigenfunctions of the unperturbed atom and $a(t)$ are time-dependent to describe the effect of the perturbation $\mathcal{H}_I$. By inserting this wave function into the equation of motion

$$i\hbar \frac{\partial \psi(\boldsymbol{r}, t)}{\partial t} = \left[\mathcal{H}_0 + \mathcal{H}_I(t)\right] \psi(\boldsymbol{r}, t) \tag{3}$$

one obtain the differential equations for the coefficients a_n

$$i\hbar\frac{\mathrm{d}a_n}{\mathrm{d}t} = -\mathcal{E}(t)\sum_m e^{-i(\epsilon_m-\epsilon_n)t}\,\langle n|d|m\rangle\,a_m. \tag{4}$$

We define $\epsilon_{mn} = \epsilon_m - \epsilon_n$ the difference between the energy levels and $d_{nm} = \langle n|d|m\rangle$ the dipole matrix element. Inserting in (4) a monochromatic light field

$$\mathcal{E}(t) = \frac{1}{2}\mathcal{E}(\omega)\left(e^{-i\omega t} + \text{c.c.}\right) \tag{5}$$

yields the coupled differential equations

$$i\hbar\frac{\mathrm{d}a_1}{\mathrm{d}t} = -d_{12}\frac{\mathcal{E}(\omega)}{2}\left[e^{-i(\omega+\epsilon_{21})t} + e^{i(\omega-\epsilon_{21})t}\right]a_2, \tag{6}$$

$$i\hbar\frac{\mathrm{d}a_2}{\mathrm{d}t} = -d_{21}\frac{\mathcal{E}(\omega)}{2}\left[e^{-i(\omega-\epsilon_{21})t} + e^{i(\omega+\epsilon_{21})t}\right]a_1. \tag{7}$$

These equations are called the optical Bloch equations. Assuming that the frequency of the light field is near resonance ($\omega \approx \epsilon_{12}$) the Bloch equations can be simplified. In this case, the part with $\omega - \epsilon_{21}$ describes a very slow, nearly time independent oscillation. On the contrary, the other part with $\omega + \epsilon_{21}$ shows a fast oscillation. While the slow varying part leads to a resonant contribution, the fast varying part is nonresonant and can therefore be neglected. This approximation is the so called rotating wave approximation (RWA) and simplifies the optical Bloch equations to

$$i\hbar\frac{\mathrm{d}a_1}{\mathrm{d}t} = -\frac{d_{12}\mathcal{E}(\omega)}{2}e^{i(\omega-\epsilon_{21})t}a_2, \tag{8}$$

$$i\hbar\frac{\mathrm{d}a_2}{\mathrm{d}t} = -\frac{d_{21}\mathcal{E}(\omega)}{2}e^{-i(\omega-\epsilon_{21})t}a_1. \tag{9}$$

Now, one can insert the two differential equations into each other and find a differential equation closed in a_2 or a_1. In the following we solve this equation and find the splitting of the energy levels for two cases:

(i) Exact resonance $\omega = \epsilon_{21}$

(ii) Detuning of the light field frequency to the transition energy of $\nu = \omega - \epsilon_{21}$

Case of exact resonance: Assuming exact resonance completely eliminates the exponential functions leaving a differential equation for a_2 as

$$\frac{\mathrm{d}^2a_2}{\mathrm{d}t^2} = -\left|\frac{d_{12}\mathcal{E}(\omega)}{2\hbar}\right|^2 a_2 = -\frac{\omega_R^2}{4}a_2 \tag{10}$$

while using $d_{21} = d_{12}^*$ and $\omega_R = \frac{|d_{21}\boldsymbol{\mathcal{E}}(t)|}{\hbar}$ the Rabi frequency. The solution to this differential equation is easily attained as

$$a_2(t) = a_2(0)e^{\pm\omega_R t/2} \tag{11}$$

which results into an atomic wave function

$$\psi(\boldsymbol{r},t) = a_1(0)e^{-i(\epsilon_1\pm\omega_R/2)t}\psi_1(\boldsymbol{r}) + a_2(0)e^{-i(\epsilon_2\pm\omega_R/2)t}\psi_2(\boldsymbol{r}). \tag{12}$$

As one can see in figure 1, the energy levels ϵ_1 and ϵ_2 in (2) are now split up into $\epsilon_1 \pm \omega_R/2$ and $\epsilon_2 \pm \omega_R/2$. This also leads to a splitting of the transition energy ϵ_{21} which is also known as the Mollow triplet

$$\epsilon_{21} \rightarrow \begin{cases} \epsilon_{21} & +\omega_R \\ \epsilon_{21} & \\ \epsilon_{21} & -\omega_R \end{cases}. \tag{13}$$

It is important to mention that the field strength has to be high enough to observe the so called Rabi sidebands $\epsilon_{21} \pm \omega_R$. This is caused by the relatively small value of the dipole moment which is multiplied with the electric field to get the Rabi frequency and the line broadening that has to be exceeded in real systems.

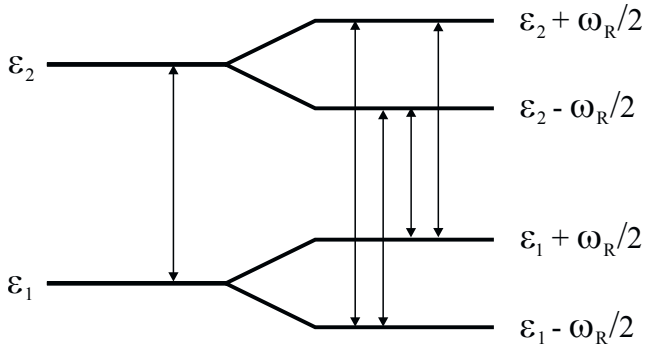

Figure 1: Schematic drawing of the frequency scheme of a two-level system with and without light field induced level splitting in the resonant part with $\omega = \epsilon_{21}$. The arrows show the optical transitions and the emergence of the Rabi sidebands in a external light field [1].

Case of finite detuning: A splitting of the energy levels can also be obtained, if the external light field is not in resonance with the transition energy. In that case, one gets a detuning $\nu = \epsilon_{21} - \omega$ and the Bloch equations in (8) and (9) become

$$\frac{\mathrm{d}a_1}{\mathrm{d}t} = ie^{-i\nu t}\frac{d_{12}\mathcal{E}(\omega)}{2\hbar}a_2, \tag{14}$$

$$\frac{\mathrm{d}a_2}{\mathrm{d}t} = ie^{i\nu t}\frac{d_{21}\mathcal{E}(\omega)}{2\hbar}a_1. \tag{15}$$

These equations can again be brought into differential equations closed in a_1 and a_2. In the case of a_1 the equation is

$$\frac{\mathrm{d}^2a_1}{\mathrm{d}t^2} = -i\nu\frac{\mathrm{d}a_1}{\mathrm{d}t} - \frac{\omega_R^2 a_1}{4}. \tag{16}$$

The solution has the form

$$a_1(t) = a_1(0)e^{i\Omega t} \tag{17}$$

with $\Omega = -\frac{\nu}{2} \pm \frac{1}{2}\sqrt{\nu^2 + \omega_R^2}$. The solution for a_2 is obtained similarly and the atomic wave function then is

$$\psi(\boldsymbol{r}, t) = a_1(0)e^{-i(\epsilon_1 - \Omega)t}\psi_1(\boldsymbol{r}) + a_2(0)e^{-i(\epsilon_2 + \Omega)t}\psi_2(\boldsymbol{r}). \tag{18}$$

In figure 2 the splitting of the levels can be seen as well as the Mollow triplet

$$\epsilon_{21} \rightarrow \begin{cases} \epsilon_{21} & -\nu & +\sqrt{\nu^2+\omega_R^2} \\ \epsilon_{21} & -\nu & \\ \epsilon_{21} & -\nu & -\sqrt{\nu^2+\omega_R^2} \end{cases}. \tag{19}$$

For $\nu \gg \omega_R$ one can approximate

$$\sqrt{\nu^2+\omega_R^2} \approx \nu\left(1+\frac{1}{2}\left(\frac{\omega_R}{\nu}\right)^2\right) = \nu + \frac{1}{2}\frac{\omega_R^2}{\nu} \tag{20}$$

and the Mollow triplet simplifies to

$$\epsilon_{21} \rightarrow \begin{cases} \epsilon_{21} & & +\frac{1}{2}\frac{\omega_R^2}{\nu} \\ \epsilon_{21} & -\nu & \\ \epsilon_{21} & -2\nu & -\frac{1}{2}\frac{\omega_R^2}{\nu} \end{cases}. \tag{21}$$

One can see, that the upper sideband $\epsilon_{21} + \frac{1}{2}\frac{\omega_R^2}{\nu}$ is closest to resonance. This transistion is the one that is observed in experiment as a small blueshift depending on the intensity of the light field. The other transitions are much farer away from the resonance and will not be observed in experiment [1].

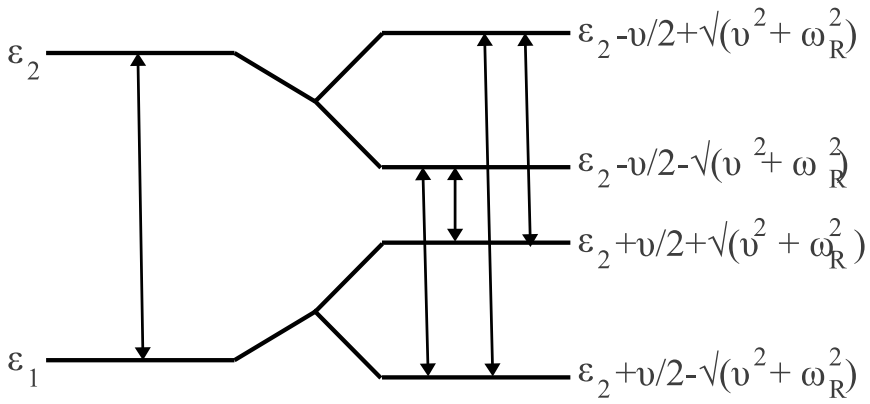

Figure 2: Schematic drawing of a two-level system without and with light field induced level splitting in the detuned case. The arrows show the optical transitions and one can see, that the upper sideband transition is closest to the transition energy without light field.

2.2 Description in second quantization

To be able to compare the results of the two-level atom with the excitonic optical Stark effect, it is convenient to describe the system in second quantization. In this chapter it is shown, that an evaluation of the polarization using a second quantization Hamiltonian describes the same system that is described above.
The Hamiltonian of a two-level atom in an external light field in second quantization is

$$\mathcal{H} = \sum_{j=1,2} \hbar\epsilon_j a_j^\dagger a_j - \left[d_{21}\mathcal{E}(t)a_2^\dagger a_1 + \text{h.c.}\right]. \tag{22}$$

Now, a_j and $a_j^\dagger$ are the annihilation and creation operator for an electron in level j with energy ϵ_j. Using this notation, electron population in level j is given $n_j = \left\langle a_j^\dagger a_2 j \right\rangle$. Since one assumes a two-level atom, the total population is given $n_1 + n_2 = 1$ and one defines $n = n_2$ for simplicity. While the densities are the diagonal elements of the density matrix, the polarization is given by the off-diagonal elements as $P = \left\langle a_1^\dagger a_2 \right\rangle$. Using the Heisenberg equation one gets the equations of motion for these two quantities as

$$\frac{\mathrm{d}P}{\mathrm{d}t} = \frac{i}{\hbar}\left[\mathcal{H}, P\right] + \frac{\partial P}{\partial t} = -i\epsilon P + \frac{id_{21}}{\hbar}\mathcal{E}_p\left(1-2n\right), \tag{23}$$

$$\frac{\mathrm{d}n}{\mathrm{d}t} = \frac{i}{\hbar}\left(d_{21}\mathcal{E}_p P^* - \text{h.c.}\right). \tag{24}$$

These equations are completely coherent, because damping was neglected and a conserved quantity

$$K = (1-2n)^2 + 4\left|P\right|^2 \tag{25}$$

exists as can be easily verified. By assuming, that there is no electron population in the upper state and no polarization as initial condition ($n = 0$,d $P = 0$ and therefore $K = 1$), one finds a direct relation between density and polarization

$$n = \frac{1}{2}\left(1 \pm \sqrt{1 - 4\left|P\right|^2}\right). \tag{26}$$

This means, that the population is completely determined by the polarization, i.e. all excitations have to be considered virtual. While the light field is switched on, the excitation occurs without delay as well as it vanishes when the field is switched off. If there where real excitations, the excited electrons would live even after the field is off and would decay with a characteristic lifetime.
The splitting of the energy levels is found by evaluating (23) and (24) in frequency space. Assuming $\mathcal{E}(t) = \mathcal{E}_p \exp(-i\omega_p t)$ and performing the Fourier transform

$$\widetilde{A}(\omega) = \int \mathrm{d}t\; e^{i\omega t} A(t) \tag{27}$$

leads to a set of equations in frequency-space

$$\left(\omega - \epsilon\right)\widetilde{P}(\omega) = -\frac{d_{21}}{\hbar}\mathcal{E}_p\left(\delta(\omega-\omega_p) - 2\widetilde{n}(\omega-\omega_p)\right), \tag{28}$$

$$\left(-\omega - \epsilon\right)\widetilde{P}^*(\omega) = -\frac{d_{21}^*}{\hbar}\mathcal{E}_p\left(\delta(\omega+\omega_p) - 2\widetilde{n}(\omega+\omega_p)\right), \tag{29}$$

$$\omega\widetilde{n}(\omega) = \frac{1}{\hbar}\left(d_{21}^*\mathcal{E}_p\widetilde{P}(\omega+\omega_p) - d_{21}\mathcal{E}_p\widetilde{P}^*(\omega-\omega_p)\right). \tag{30}$$

By inserting (29) and (30) into (28) one obtains an equation closed in $\widetilde{P}(\omega)$ and therefore an equation describing the frequency relations

$$\left(\omega - \omega_p\right)\left[(\omega-\epsilon)(-\omega-\epsilon+2\omega_p) + 4\omega_R^2\right] = 0. \tag{31}$$

For the exact resonant part $\omega_p = \epsilon$ one finds the solution

$$\omega = \begin{cases} \epsilon & +2\omega_R \\ \epsilon & \\ \epsilon & -2\omega_R \end{cases} \tag{32}$$

and in the case of a finite detuning $\nu = \epsilon - \omega_p$ the solution yields

$$\omega = \begin{cases} \epsilon - \nu & +\sqrt{\nu^2 + 4\omega_R^2} \\ \epsilon - \nu & \\ \epsilon - \nu & -\sqrt{\nu^2 + 4\omega_R^2} \end{cases}. \tag{33}$$

These solutions match the Mollow triplets evaluated in (13) and (21). [1]

3 Excitonic optical Stark effect

Now, after examination of the optical Stark effect in a two-level atom the excitonic optical Stark effect in semiconductors can be derived. The setting is more complicated in this case, caused by the short dephasing times in semiconductors. Here, the coherence decays in a timescale of femtoseconds, but can grow larger if one observes bound states like excitons. In the best case, the coherence timescale can reach picoseconds. Thus a stationary description can no longer be applied. Instead of that one has to take dynamic effects into account, because one deals with a femtosecond experiment.
An efficient experimental method to examine the excitonic optical Stark effect is a pump-probe experiment using femtosecond pulses. In figure 3, a schematic pump-probe experiment is shown. The experiment is influenced by a strong detuned pump beam and then a short probe beam is applied to find the difference in absorption before (α_{np}) and after (α_p) the influence of the pump beam

$$\delta\alpha = \alpha_p - \alpha_{np}. \tag{34}$$

To observe a broad frequency area, the probe beam has to be short in time and in order to be distinguished from the pump pulse it propagates in a direction different then the one oft the pump beam.

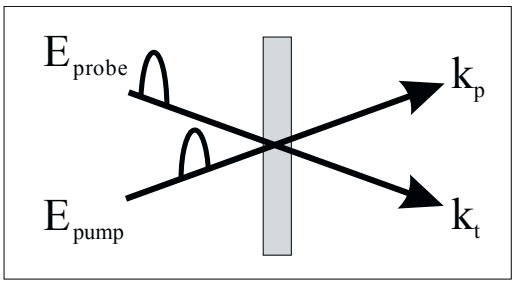

Figure 3: Schematic set-up for a pump-probe experiment [1].

3.1 Quasi stationary approximation

An overview of the effect can be obtained in a quasi stationary approximation as a first step. Although a stationary description is not justified as stated above, one can learn various characteristics. A quasi stationary approximation requires, that the variations in the amplitude of the light field are slow so that only adiabatic changes apply. Therefore one assumes the pump beam a plain wave with a constant amplitude. Solving the effect of the pump beam adiabatically allows the probe beam to be considered as perturbation.
The time dependency of the polarization P_k and the density in the conduction band $n_k = n_{c,k} =$

$1 - n_{v,k}$ can be derived from the semiconductor Bloch equations. By neglecting scattering effects due to the low densities one gets

$$\frac{\mathrm{d}P_k}{\mathrm{d}t} = -ie_k P_k - (1 - 2n_k)\,\omega_{R,k}, \tag{35}$$

$$\frac{\mathrm{d}n_k}{\mathrm{d}t} = i\left(\omega_{R_k} P_k^* - \omega_{R,k}^* P_k\right). \tag{36}$$

The energy e_k describes the exciton energy

$$\hbar e_k = \hbar\left(e_{e,k} + e_{h,k}\right) = E_g + \frac{\hbar^2 k^2}{2m} - 2\sum_{k'} V_{k-k'} n_{k'} \tag{37}$$

and the effective Rabi frequency $\omega_{R,k}$ is given as

$$\omega_{R,k} = \frac{1}{\hbar}\left(d_{cv}\mathcal{E} + \sum_{q\neq k} V_{|k-q|} P_q\right). \tag{38}$$

A comparison between the semiconductor Bloch equations and the equations of motion for the two-level atom (23) and (24) shows, that there is a nearly complete analogy. The only difference lays in the mixing of k-states in the exciton energy and the effective Rabi frequency. Nevertheless one can find the same conserved quantity K as in (25) and consequentely the equation

$$n_k = \frac{1}{2}\left(1 \pm \sqrt{1 - 4\left|P_k\right|^2}\right). \tag{39}$$

This implies a direct coherence between density and polarisation closed in k. So by considering the adiabatic approximation one can show that only the minus sign can be realized, because population inversion is not possible in this approximation and therefore $n_k \leq 1/2$ and $|P_k|^2 \leq 1/2$ must be assured.
Now, the solution for the polarization induced by the pump beam can be attained adiabatically by assuming the pump beam to be a plain wave

$$\mathcal{E}_p(t) = \mathcal{E}_p \exp(-i\omega_p t) \tag{40}$$

as it is demanded by the adiabatic approximation. Because the light field does not change in amplitude, one can assume, that the polarization will follow the time dependence of the pump beam, reducing its time dependency to

$$P_k(t) = p_k(t)e^{-i\omega_p t} \simeq p_k e^{-i\omega_p t}. \tag{41}$$

Solving (35) and (39) using this assumption yields

$$P_k(t) = \frac{(1 - 2n_k)\,\omega_{R,k}}{e_k - \omega_p} \propto e^{-i\omega_p t}. \tag{42}$$

To see the effect of the above pump-induced polarization on the probe pulse, one can use a weak probe beam with $\mathcal{E}_t(t) = \mathcal{E}_t \exp(-i\omega_t t)$ that induces a small change in polarization $P_k \to P_k + \delta P_k$. Inserting this into the semiconductor Bloch equation (35) and keeping only terms in first order yields

$$i\frac{\mathrm{d}}{\mathrm{d}t}\delta P_k = \delta e_k P_k + e_k \delta P_k + 2\delta n_k \omega_{R,k} - (1 - 2n_k)\,\delta\omega_{R,k} \tag{43}$$

with the first order changes in exciton energy, density and Rabi frequency

$$\delta e_k = -\frac{2}{\hbar}\sum_{k'} V_{k-k'}\delta n_{k'}, \tag{44}$$

$$\delta n_k = \frac{P_k\delta P_k^* + P_k^*\delta P_k}{1-2n_k}, \tag{45}$$

$$\delta\omega_{R,k} = \frac{d_{cv}\mathcal{E}_t}{\hbar}e^{-i\omega_t t} + \frac{1}{\hbar}\sum_{k'} V_{k-k'}\delta P_{k'}. \tag{46}$$

To find the solution of the change in polarization induced by the probe beam a transformation into the rotating picture is performed by $P_k = p_k \exp(-i\omega_p t)$ gaining

$$i\frac{\mathrm{d}}{\mathrm{d}t}\delta p_k = \delta e_k p_k + (e_k - \omega_p)\,\delta p_k + 2\delta n_k\omega_{R,k} - (1-2n_k)\,\delta\omega_{R,k}. \tag{47}$$

This transformation requires a redefinition of the change in the Rabi frequency as

$$\delta\omega_{R,k} \to \delta\omega_{R,k} = \frac{d_{cv}\mathcal{E}_t}{\hbar}e^{i\Delta t} + \frac{1}{\hbar}\sum_{k'} V_{k-k'}\delta p_{k'} \tag{48}$$

with $\Delta = \omega_p - \omega_t$. Although the time dependency of the pump beam was eliminated by the transformation, the change in polarization still depends on the polarization induced by the pump beam and thus one can get the influence of the pump beam on the system by analysing the probe beam. The solution of δp_k in this picture then has the form

$$\delta p_k = \delta p_k^+ e^{i\Delta t} + \delta p_k^- e^{-i\Delta t}. \tag{49}$$

Considering, that the time dependency of the field is proportional to $\exp(i\Delta t)$, δp_k^+ describes the resonant part. Therefore calculation of δp_k^+, which can be attained numerically, allows to evaluate the absorption spectrum and out of it the possible shifts in the transition energies. In figure 4 the absorption spectrum of the probe beam is plotted for this calculations. It is assumed, that the pump beam has a large detuning of $(\hbar\omega_p - E_g)/E_0 = -10$ with the gap energy E_g and the exciton binding energy E_0. The absorption is plotted versus the normalized detuning of the probe beam. It shows, that for a pump intensity $I_p = 0$ MW/cm^2 the first absorption peak lies at $-E_0$, exactly at the exciton resonance. If the intensity is increased, one finds a blueshift of this peak, what means a higher transition energy. To have a look on the formula of the upper Rabi sideband in the detuned case of the two-level atom

$$\omega = E_0 - \nu + \sqrt{\nu^2 + \omega_R^2} \tag{50}$$

with $\omega_R^2 \propto I_p$ shows that one observes the same effect and thus can specify it as a Stark effect. However, one has to mind that this model assumes full coherence and neglects damping caused by the detuning. A more accurate description is delivered by the dynamic results. [1]

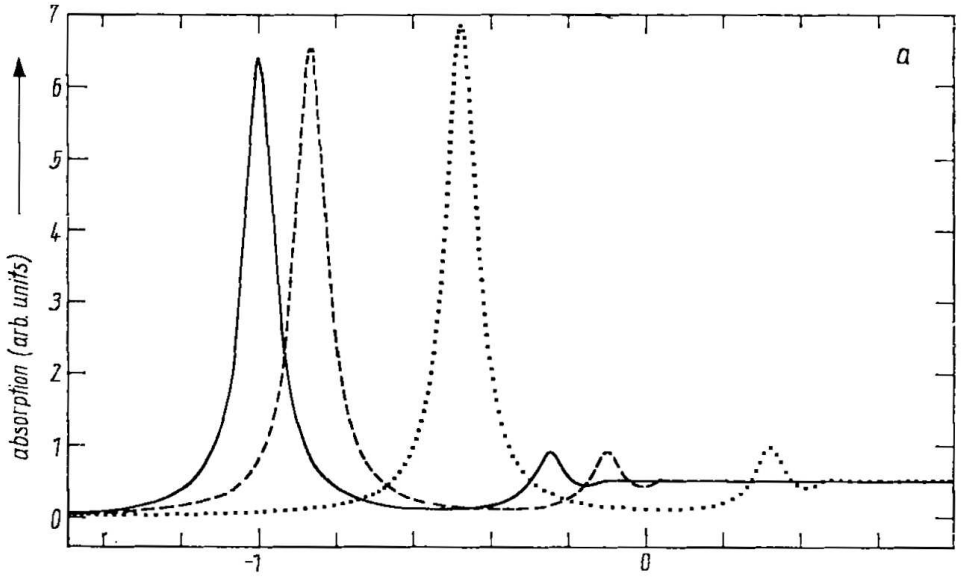

Figure 4: Numerically attained absorption spectrum in a three-dimensional semiconductor versus the normalized detuning $(\hbar\omega_t - E_g)/E_0$ of the probe beam for a normalized detuning of the pump beam of $(\hbar\omega_p - E_g)/E_0 = -10$ with $I_p = 0,\ 7.5,\ 30$ MW/cm^2 from left to right [2].

3.2 Dynamic results

While the previous sections show the optical Stark effect in stationary regimes, the dynamic results take finite pulses with specific time delays into account. So, the electric field is no longer considered to have a constant amplitude and furthermore the direction of propagation is introduced in

$$\mathcal{E}(r,t) = \mathcal{E}_p(t)e^{-i(\boldsymbol{k}_p\cdot\boldsymbol{r}+\Omega t)} + \mathcal{E}_t(t)e^{-(\boldsymbol{k}_t\cdot\boldsymbol{r}+\Omega t)}. \tag{51}$$

Since one wants to observe the change of absorption in the probe beam, the condition $\boldsymbol{k}_p \neq \boldsymbol{k}_t$ has to be fulfilled. To gain results for the absorption one has to find the polarization defined by the semiconductor Bloch equations. Here, the nonlinear terms of the order of $\mathcal{O}(n \cdot P)$ are neglected, what leads to the linear semiconductor Bloch equations

$$\hbar\left[i\frac{\partial}{\partial t} - \epsilon_k\right] P_{\boldsymbol{k}} = (2n_{\boldsymbol{k}} - 1)d_{cv}\mathcal{E}(t) - \sum_{\boldsymbol{q}\neq\boldsymbol{k}} V_{|\boldsymbol{k}-\boldsymbol{q}|}P_{\boldsymbol{q}}, \tag{52}$$

$$\hbar\frac{\partial}{\partial t}n_{\boldsymbol{k}} = i\left[d_{cv}\mathcal{E}(t)P^*_{\boldsymbol{k}} - \text{c.c.}\right]. \tag{53}$$

To find the polarization in terms of the exciton eigenfunction, (52) and (53) are transformed to real space what yields

$$i\hbar\frac{\partial}{\partial t}P(\boldsymbol{r}) = \mathcal{H}_{eh}P(\boldsymbol{r}) + d_{cv}\mathcal{E}(t)\left[2n(\boldsymbol{r}) - \delta(r)\right] \tag{54}$$

$$\hbar\frac{\partial}{\partial t}n(\boldsymbol{r}) = i,\left[d_{cv}\mathcal{E}(t)P^*(-\boldsymbol{r}) - \text{c.c.}\right] \tag{55}$$

with the Wannier Hamiltonian

$$\mathcal{H}_{eh} = \epsilon_g - \frac{\hbar^2\nabla^2}{2m_r} - V(r) \tag{56}$$

which describes the exciton energy. Now, (54) and (55) are multiplicated with the exciton eigenfunction $\psi_\lambda(\boldsymbol{r})$ and integrated over the space as

$$\int \mathrm{d}\boldsymbol{r}\ \psi_\lambda(\boldsymbol{r}) i\hbar \frac{\partial}{\partial t} P(\boldsymbol{r}) = \int \mathrm{d}\boldsymbol{r}\ \psi_\lambda(\boldsymbol{r}) \mathcal{H}_{eh} P(\boldsymbol{r}) \tag{57}$$

$$+ \int \mathrm{d}\boldsymbol{r}\ \psi_\lambda(\boldsymbol{r}) d_{cv} \mathcal{E}(t) \left[2n(\boldsymbol{r}) - \delta(r)\right], \tag{58}$$

$$\int \mathrm{d}\boldsymbol{r}\ \psi_\lambda(\boldsymbol{r}) \hbar \frac{\partial}{\partial t} n(\boldsymbol{r}) = \int \mathrm{d}\boldsymbol{r}\ \psi_\lambda(\boldsymbol{r}) i \left[d_{cv} \mathcal{E}(t) P^*(-\boldsymbol{r}) - \text{c.c.}\right]. \tag{59}$$

The solution to these two equations provides equations closed in λ, what means that the effect can be described for different exciton states separately with

$$i\hbar \frac{\partial}{\partial t} P_\lambda = \hbar \epsilon_\lambda P_\lambda + d_{cv} \mathcal{E}(t) \left[2n_\lambda - \psi_\lambda(r=0)\right], \tag{60}$$

$$\hbar \frac{\partial}{\partial t} n_\lambda = i d_{cv} \mathcal{E}(t) P_\lambda^* - i d_{cv} \mathcal{E}(t) P_\lambda. \tag{61}$$

In a next step, a transformation into rotation picture is performed and the dependency of $\psi(r=0)$ is eliminated in the polarization by defining

$$P_\lambda = \psi_\lambda(r=0) e^{-i\Omega t} p_\lambda. \tag{62}$$

The density in the upper level n_λ is changed into the difference in density between upper and lower level $w_\lambda = n_{1,\lambda} - n_{2,\lambda}$ as well as the dependency of $\psi(r=0)$ is eliminated by

$$w_\lambda = \psi_\lambda(r=0)\ (1 - 2n_\lambda). \tag{63}$$

Additionally a damping γ for the polarization and Γ for the density is introduced, which yields

$$\frac{\partial}{\partial t} p_\lambda = \left[i(\epsilon_\lambda - \Omega) + \gamma\right] p_\lambda + i \frac{d_{cv}}{\hbar} \left[\mathcal{E}_p(t) e^{-i\boldsymbol{k}_p \cdot \boldsymbol{r}} + \mathcal{E}_t(t) e^{-i\boldsymbol{k}_t \cdot \boldsymbol{r}}\right] w_\lambda, \tag{64}$$

$$\frac{\partial}{\partial t} w_\lambda = -\Gamma(w_\lambda - 1) - i \frac{2d_{cv}}{\hbar} \left[\mathcal{E}_p(t) e^{-i\boldsymbol{k}_p \cdot \boldsymbol{r}} + \mathcal{E}_t(t) e^{-i\boldsymbol{k}_t \cdot \boldsymbol{r}}\right] p_\lambda^* + i \frac{2d_{cv}^*}{\hbar} \left[\mathcal{E}_p^*(t) e^{i\boldsymbol{k}_p \cdot \boldsymbol{r}} + \mathcal{E}_t^*(t) e^{-i\boldsymbol{k}_t \cdot \boldsymbol{r}}\right] p_\lambda. \tag{65}$$

Now, one has to perform a set of approximations and assumptions to simplify the problem. Thus the probe pulse is considered to be short, what allows to approximate the pulse as a delta function

$$\mathcal{E}_t(t) \simeq \mathcal{E}_t \delta(t - t_t). \tag{66}$$

Here, it is important to remember, that one is interested only in the part that is propagating in probe beam direction $\exp(i\boldsymbol{k}_t \cdot \boldsymbol{r})$. If the probe beam is also considered to be weak, one can neglect every but the first order in $\mathcal{E}_t$. In the next steps, one finds, that if one is interested only in the first order changes in polarization, all orders higher then second order in $\mathcal{E}_p$ can be neglected as well. The equation for the polarization is now obtained by integrating (64) over the time as

$$p_\lambda(t) \simeq i \frac{d_{cv}}{\hbar} \mathcal{E}_t e^{-i\boldsymbol{k}_t \cdot \boldsymbol{r}} e^{-[i(\epsilon_\lambda - \Omega) + \gamma](t - t_t)} w_\lambda(t_{t-}) \Theta(t - t_t) + \underbrace{i \frac{d_{cv}}{\hbar} e^{-i\boldsymbol{k}_p \cdot \boldsymbol{r}} \int_{-\infty}^{t} \mathrm{d}t' e^{-[i(\epsilon_\lambda - \Omega) + \gamma](t - t_t)} \mathcal{E}_p(t') w_\lambda(t')}_{p_\lambda(t < t_t)} \tag{67}$$

where the first line shows the part that occurs after the appliance of the probe beam contrary to the second line, that also occurs prior to that. Here, $w_\lambda(t_{t\_})$ defines the difference of densities just before the probe pulse of the duration $t_{t+} - t_{t-}$ is applied by assuming

$$w_\lambda(t_t) \simeq w_\lambda(t_{t\_}) + \mathcal{O}(\mathcal{E}_t). \tag{68}$$

The second line itself is dependent on the difference of densities $w_\lambda(t)$. In first order of $\mathcal{E}_t$, $w_\lambda(t)$ has a component proportional to $\exp(i\boldsymbol{k}_t \cdot \boldsymbol{r})$, which leads to a term in the polarization

$$p_\lambda(t_{t\_}) \propto e^{i(\boldsymbol{k}_t - \boldsymbol{k}_p)\cdot \boldsymbol{r}}. \tag{69}$$

This can be interpreted as a grating formed by the two pulses, which scatters parts of the pump beam into the probe beam direction, even before the arrival of the probe beam on the detector. The effect leads to oscillations in the pump-probe signal, as one will later see.
To solve (67) in whole, one also needs $w_\lambda(t)$, which can similarly be written as

$$\begin{aligned} w_\lambda(t) \simeq 1 &- i\frac{2d_{cv}}{\hbar} e^{-\Gamma(t-t_t)} \mathcal{E}_t e^{-i\boldsymbol{k}_t\cdot\boldsymbol{r}} p^*_\lambda(t_{t\_})\Theta(t-t_t) + i\frac{2d^*_{cv}}{\hbar} e^{-\Gamma(t-t_t)} \mathcal{E}^*_t e^{i\boldsymbol{k}_t\cdot\boldsymbol{r}} p_\lambda(t_{t\_})\Theta(t-t_t) \\ &- i\frac{2d_{cv}}{\hbar}\int_{-\infty}^{t} \mathrm{d}t'\ e^{-\Gamma(t-t')}\mathcal{E}_p(t') e^{-i\boldsymbol{k}_p\cdot\boldsymbol{r}} p^*_\lambda(t') + i\frac{2d^*_{cv}}{\hbar}\int_{-\infty}^{t} \mathrm{d}t'\ e^{-\Gamma(t-t')}\mathcal{E}^*_p(t') e^{i\boldsymbol{k}_p\cdot\boldsymbol{r}} p_\lambda(t'). \end{aligned} \tag{70}$$

Now, inserting (70) in (67) and iteratively inserting the polarization again by considering only first order in $\mathcal{E}_t$ and second order in $\mathcal{E}_p$ yields

$$\begin{aligned} p_\lambda(t) \simeq\ & i\frac{d_{cv}}{\hbar}\mathcal{E}_t e^{-i\boldsymbol{k}_t\cdot\boldsymbol{r}} e^{-[i(\epsilon_\lambda-\Omega)+\gamma](t-t_t)} w_\lambda(t_{t\_})\Theta(t-t_t) \\ &+ 2\frac{d^2_{cv}}{\hbar^2}\mathcal{E}_t e^{-i(\boldsymbol{k}_t+\boldsymbol{k}_p)\cdot\boldsymbol{r}} p^*_\lambda(t_{t\_}) \int_{t_t}^{t} \mathrm{d}t' e^{-[i(\epsilon_\lambda-\Omega)+\gamma](t-t_t)} e^{-\Gamma(t'-t_t)}\mathcal{E}_p(t')\Theta(t-t_t) \\ &- i\frac{2d_{cv}}{\hbar}\frac{|d_{cv}|^2}{\hbar^2}\mathcal{E}_t e^{-i\boldsymbol{k}_t\cdot\boldsymbol{r}} \int_{t_t}^{t} \mathrm{d}t' e^{-[i(\epsilon_\lambda-\Omega)+\gamma](t-t')}\mathcal{E}_p(t') \\ &\times \int_{t_t}^{t'} \mathrm{d}t'' e^{-\Gamma(t'-t'')}\mathcal{E}^*_p(t'') e^{-[i(\epsilon_\lambda-\Omega)+\gamma](t''-t_t)}\Theta(t-t_t). \end{aligned} \tag{71}$$

This expression shows the first order change in the polarization induced by the pump beam. Lower orders in $\mathcal{E}_p$ would not show any effects induced by the pump beam, while higher orders are assumed to have lesser influence. So, one can use this formula to calculate the susceptibility

$$\chi_\lambda(\omega) = \frac{\mathcal{P}_\lambda(\omega)}{\mathcal{E}_t(\omega)}. \tag{72}$$

Since the frequency dependency of the polarization is needed, a Fourier transform is performed with

$$\mathcal{P}_\lambda(\omega) = \int \mathrm{d}t\ e^{i\omega t}\mathcal{P}_\lambda(t) = \int \mathrm{d}t\ e^{i(\omega-\Omega)t} p_\lambda(t) \tag{73}$$

$$= \int_0^\infty \mathrm{d}t\ e^{i(\omega-\Omega)t} p_\lambda(t+t_t) e^{-i(\omega-\Omega)t_t}. \tag{74}$$

In addition, the electric field of the probe beam is needed in frequency space, which is given by

$$\mathcal{E}_t(\omega) = \int \mathrm{d}t\ e^{i\omega t}\mathcal{E}_t(t) \simeq \mathcal{E}_t e^{i(\omega-\Omega)t_t} e^{-i\boldsymbol{k}_t\cdot\boldsymbol{r}}. \tag{75}$$

The susceptibility then yields

$$\begin{aligned}\chi_\lambda(\omega) \simeq i\frac{d_{cv}}{\hbar}\frac{1}{\gamma - i(\omega-\epsilon_\lambda)}\Big[&w_\lambda(t_{t\_}) \\ &- 2\frac{|d_{cv}|^2}{\hbar^2}\int_{-\infty}^{t_t}\mathrm{d}t'\ e^{[i(\epsilon_\lambda-\Omega)-\gamma](t_t-t')}\mathcal{E}_p^*(t')\int_0^\infty \mathrm{d}t\ e^{[i(\omega-\Omega)-\Gamma]t}\mathcal{E}_p(t+t_t) \\ &- 2\frac{|d_{cv}|^2}{\hbar^2}\int_0^\infty \mathrm{d}t\ e^{i(\omega-\Omega)t}\mathcal{E}_p(t+t_t)\int_0^t \mathrm{d}t'\ e^{-\Gamma(t-t')}e^{-[i(\epsilon_\lambda-\Omega)+\gamma]t'}\mathcal{E}_p^*(t'+t_t)\Big].\end{aligned} \tag{76}$$

To discuss this final formula for the susceptibility, in a first step one assumes a constant pump beam. In a second step, the pump beam is considered a Gaussian that varies slowly. Then in a final step, the whole attained susceptibility is considered to give a fully dynamic description [1].

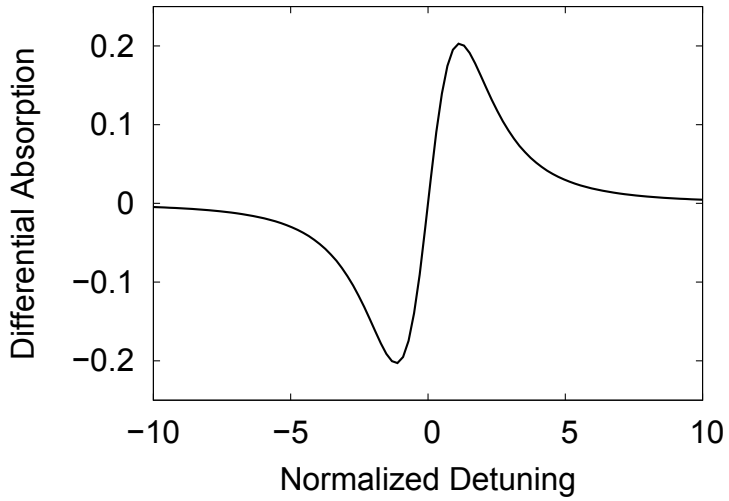

Figure 5: Differential Absorption $\delta\alpha$ over the normalized detuning, both in arbitrary units for a constant pump beam $\mathcal{E}_p = \text{const}$.

Constant pump beam: The change in susceptibility $\delta\chi$ caused by a pump beam in a slow varying or constant case is generally described by the last line in (76). Considering slow variation $\mathcal{E}_p(t') \approx \mathcal{E}_p(t)$ allows to approximate this line as

$$\begin{aligned}\delta\chi &= -2\frac{|d_{cv}|^2}{\hbar^2}\int_0^\infty \mathrm{d}t\ e^{i(\omega-\Omega)t}\mathcal{E}_p(t+t_t)\int_0^t \mathrm{d}t'\ e^{-\Gamma(t-t')}e^{-[i(\epsilon_\lambda-\Omega)+\gamma]t'}\mathcal{E}_p^*(t'+t_t)\Big] \\ &\simeq -i\frac{2\,|d_{cv}|^2}{\hbar^2}\frac{1}{\omega-\Omega}\int_0^\infty \mathrm{d}t\ e^{-[i(\epsilon_\lambda-\omega)+\gamma]t}\,|\mathcal{E}_p(t+t_t)|^2\,.\end{aligned} \tag{77}$$

The change in absorption $\delta\alpha = \alpha_p - \alpha_{np}$ (differential absorption), that is measured in experiment is then given as

$$\delta\alpha(\omega) = -\Im\left[\frac{d_{cv}^*}{\hbar}\delta\chi_\lambda(\omega)\right] \simeq \frac{|d_{cv}|^4}{\hbar^4}\frac{2}{\Omega-\epsilon_\lambda}\Im\left[\int_0^\infty \mathrm{d}t\ \frac{|E_p(t+t_t)|^2}{\gamma - i(\omega-\epsilon_\lambda)}e^{-[i(\epsilon_\lambda-\omega)+\gamma]t}\right]. \tag{78}$$

In the case of $\mathcal{E}_p = \text{const.}$ the equation simplifies to

$$\delta\alpha(\omega) \propto -\frac{|\mathcal{E}_p|^2}{\epsilon_\lambda - \Omega_p}\frac{2\gamma(\epsilon_\lambda-\omega)}{\left[(\epsilon_\lambda-\omega)^2+\gamma^2\right]^2} \tag{79}$$

which is shown in figure 5. The absorption on the left side of the resonance frequency decreases while the absorption on the right side increases. This means, that the absorption is shifted to the right, i.d. a blueshift of the resonance and thus a Stark shift is observed [1].

Slow varying Gaussian: To describe the pump beam as a Gaussian, but still assume to have slow variations (79) has to be evaluated for

$$\mathcal{E}_p(t) = \mathcal{E}_0 e^{-\frac{(t-t_p)^2}{2\sigma^2}}. \tag{80}$$

This can be performed for 120 fs pulses in the case of simultaneous pump and probe beam in figure 6(a) and in the case of a delay of $t_t - t_p = 50$ fs in figure 6(b). One finds again a differential absorption that describes a blueshift of the resonance and one also observes, that the shift decreases with increasing time delay. Here, it is obvious, that the optical Stark effect in semiconductors is an effect in femtosecond time scale because it decays very fast [1].

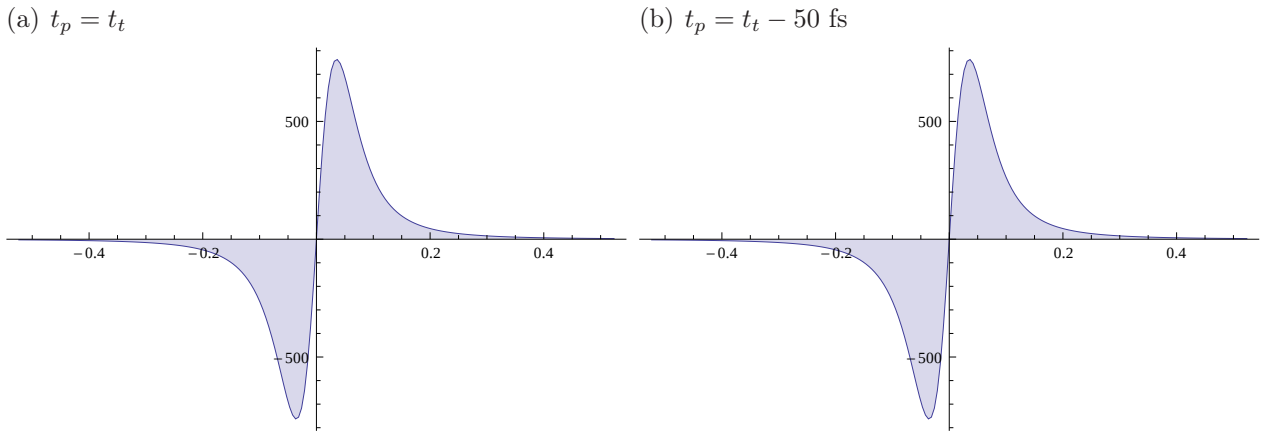

Figure 6: The differential absorption $\delta\alpha$ over the normalized detuning $(\omega - \epsilon_\lambda)/\sigma$ for a pulse length of 120 fs and a pump pulse detuning of -10 below the resonance. The shift for $t_p = t_t$ (a) is about three times larger than for $t_p = t_t - 50$ fs (b).

Dynamic description: In this final step, the whole susceptibility in (76) is considered. This enables to examine pump probe delays as in the slow varying case on the one hand, but on the other hand a probe pump delay can be examined. In figure 7 the differential absorption for 120 fs pulses is plotted. The upmost plot considers simultaneous pump and probe beam and shows again a blueshift as one expects for an optical Stark shift. The lowermost plot considers

a probe pump delay of $t_p = t_t - 500$ fs, i.e. the probe beam emerges before the pump beam. Here, one finds a symmetric oscillating change in the absorption. This is no Stark effect but can be explained as an effect of the grating that is created with the two pulses and leads to the scattering the pump pulse into the probe pulse direction. In the uppermost plot for $t_p = t_t$, we obtain again a blueshift in the absorption similar to the result in figure 5.

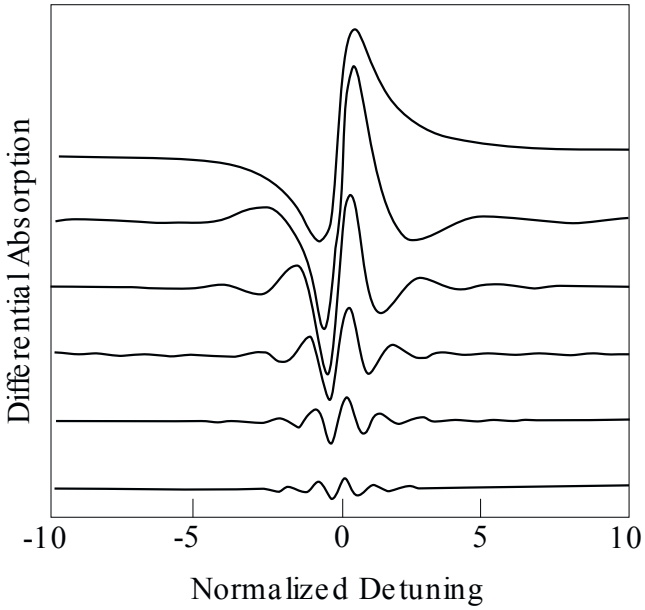

Figure 7: Differential absorption spectrum with probe pulse before pump pulse over the normalized detuning $(\omega - \epsilon_\lambda)/\sigma$ with the FWHM of the pump pulse $\sigma = 120$ fs. The detuning of the pump puls is -10 below the resonance. The upmost curve shows no time delay between pump and pulse beam. From top to bottom the delay increases by 100 fs for each curve until a pump probe delay $t_p - t_t = -500$ fs for the lowermost curve [1].

4 Conclusion

In conclusion, the optical Stark effect, known from the two-level atom can be adopted to a semiconductor and evaluated quasi-stationary as well as dynamic. In figure 8, experimental results are shown. The leftmost curve shows the absorption spectrum without pumping. For increasing pump intensity, the peaks are obviously blueshifted as long as the intensity does not become too high. In this case, the oscillator strength of the continuum state becomes stronger then the oscillator strength of the bound exciton states and thus the peaks vanish. This experiment shows, that the excitonic optical Stark shift can be experimental observed and the theoretical description captures its basic features. It is even possible to predict other dynamic effects like the scattering of the pump beam into probe beam direction.
Still, one has to take into consideration, that one can only predict the first order changes with this method, because higher orders are neglected. In the semiconductor Bloch equations, the nonlinear terms and the scattering terms are neglected as well. So, our calculations give a qualitative description of the optical Stark effect in a semiconductor, but non linear effects, the role of continuum states, etc. have not been considered here.

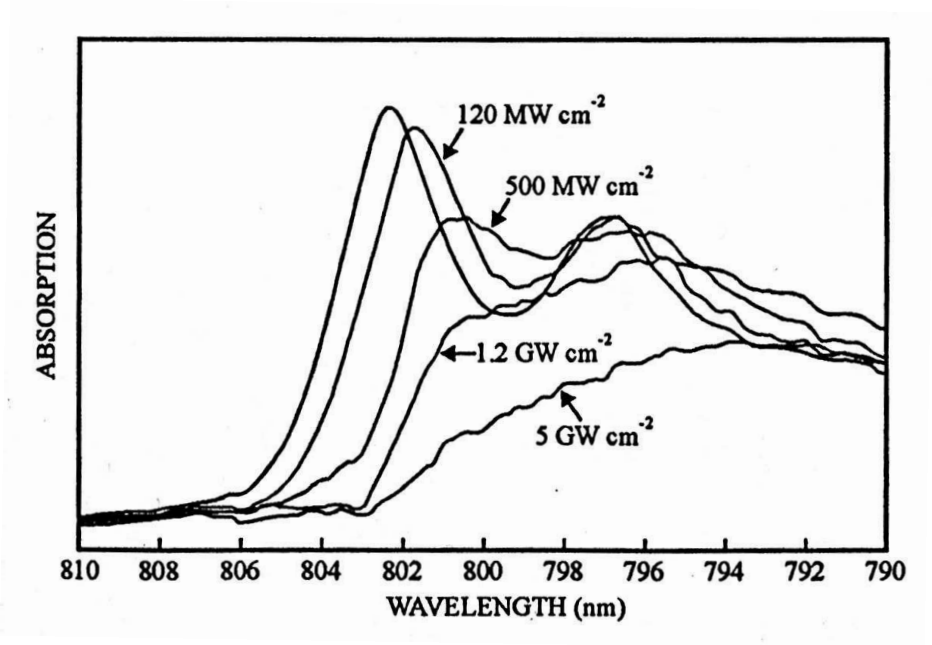

Figure 8: Experimental Absorption using 400 fs pulses for different pump pulse intensities [3].

List of Figures

References

[1] Hartmut Haug and Stephan W. Koch. *Quantum Theory of the Optical and Electronic Properties of Semiconductors*. World Scientific, London, 4. edition, 2004.

[2] C. Ell, J. F. Müller, K. El Sayed, L. Banyai, and H. Haug. Evaluation of the hartree-fock theory of the excitonic optical stark effect. *physica status solidi (b)*, 150(2):393–399, 1988.

[3] Wilfried Schäfer and Martin Wegener. *Semiconductor optics and transport phenomena*. Springer, Berlin; Heidelberg, 2002.